# UC Irvine
## UC Irvine Previously Published Works

**Title**

α3* Nicotinic Acetylcholine Receptors in the Habenula-Interpeduncular Nucleus Circuit Regulate Nicotine Intake

**Permalink**

https://escholarship.org/uc/item/98d9z84v

**Journal**

Journal of Neuroscience, 41(8)

**ISSN**

0270-6474

**Authors**

Elayouby, Karim S
Ishikawa, Masago
Dukes, Angeline J
et al.

**Publication Date**

2021-02-24

**DOI**

10.1523/jneurosci.0127-19.2020

Peer reviewed

Behavioral/Cognitive

# α3∗ Nicotinic Acetylcholine Receptors in the Habenula-Interpeduncular Nucleus Circuit Regulate Nicotine Intake

**Karim S. Elayouby,**[1] **Masago Ishikawa,**[1] **Angeline J. Dukes,**[2] ⬤**Alexander C. W. Smith,**[1] **Qun Lu,**[3] ⬤**Christie D. Fowler,**[2] **and Paul J. Kenny**[1]

[1]Nash Family Department of Neuroscience, Icahn School of Medicine at Mount Sinai, New York, New York 10029, [2]Department of Neurobiology and Behavior, University of California Irvine, Irvine, California 92697, and [3]Department of Molecular Medicine, Scripps Research, Jupiter, Florida 33458

Allelic variation in *CHRNA3*, the gene encoding the α3 nicotinic acetylcholine receptor (nAChR) subunit, increases vulnerability to tobacco dependence and smoking-related diseases, but little is known about the role for α3-containing (α3∗) nAChRs in regulating the addiction-related behavioral or physiological actions of nicotine. α3∗ nAChRs are densely expressed by medial habenula (mHb) neurons, which project almost exclusively to the interpeduncular nucleus (IPn) and are known to regulate nicotine avoidance behaviors. We found that *Chrna3*[tm1.1Hwrt] hypomorphic mice, which express constitutively low levels of α3∗ nAChRs, self-administer greater quantities of nicotine (0.4 mg kg$^{-1}$ per infusion) than their wild-type littermates. Microinfusion of a lentivirus vector to express a short-hairpin RNA into the mHb or IPn to knock-down *Chrna3* transcripts markedly increased nicotine self-administration behavior in rats (0.01–0.18 mg kg$^{-1}$ per infusion). Using whole-cell recordings, we found that the α3β4∗ nAChR-selective antagonist α-conotoxin AuIB almost completely abolished nicotine-evoked currents in mHb neurons. By contrast, the α3β2∗ nAChR-selective antagonist α-conotoxin MII only partially attenuated these currents. Finally, micro-infusion of α-conotoxin AuIB (10 μM) but not α-conotoxin MII (10 μM) into the IPn in rats increased nicotine self-administration behavior. Together, these data suggest that α3β4∗ nAChRs regulate the stimulatory effects of nicotine on the mHb-IPn circuit and thereby regulate nicotine avoidance behaviors. These findings provide mechanistic insights into how *CHRNA3* risk alleles can increase the risk of tobacco dependence and smoking-related diseases in human smokers.

*Key words:* addiction; CHRNA3; habenula; interpeduncular nucleus; nicotine; self-administration

---

### Significance Statement

Allelic variation in *CHRNA3*, which encodes the α3 nicotinic acetylcholine receptor (nAChR) subunit gene, increases risk of tobacco dependence but underlying mechanisms are unclear. We report that *Chrna3* hypomorphic mice consume greater quantities of nicotine than wild-type mice and that knock-down of *Chrna3* gene transcripts in the habenula or interpeduncular nucleus (IPn) increases nicotine intake in rats. α-Conotoxin AuIB, a potent antagonist of the α3β4 nAChR subtype, reduced the stimulatory effects of nicotine on habenular neurons, and its infusion into the IPn increased nicotine intake in rats. These data suggest that α3β4 nAChRs in the habenula-IPn circuit regulate the motivational properties of nicotine.

---

## Introduction

Nicotine is considered the major component of tobacco responsible for addiction in cigarette smokers (Stolerman and Jarvis, 1995). Nicotine exerts its actions in the brain through nicotinic

acetylcholine receptors (nAChRs), with those containing the α4 and β2 subunits (denoted as α4β2∗ nAChRs) being the most prevalent in the central nervous system. α4β2∗ nAChRs in the ventral tegmental area (VTA) regulate the stimulatory effects of nicotine on mesoaccumbens dopamine transmission, an action considered critical for the reinforcing properties of the drug (Maskos et al., 2005; Liu et al., 2012). Allelic variation in the *CHRNA5-CHRNA3-CHRNB4* gene cluster located in chromosome region 15q25, which encodes the α5, α3, and β4 nAChR subunits, respectively, increases the risk of tobacco dependence and smoking-related diseases (Amos et al., 2008; Berrettini et al., 2008). In particular, variation in *CHRNA3* has been repeatedly associated with vulnerability to tobacco dependence and the number of cigarettes smoked per day, with the rs1051730 single nucleotide polymorphism (SNP) being strongly implicated

(Amos et al., 2008; Marques-Vidal et al., 2011; Ware et al., 2011). Little is currently known about the mechanisms by which $\alpha$3* nAChRs regulate the motivational properties of nicotine to influence tobacco dependence vulnerability in this manner.

In contrast to $\alpha$4 and $\beta$2 nAChR subunits, which are widely distributed throughout the mammalian brain, $\alpha$3, $\alpha$5, and $\beta$4 nAChR subunits show far more restricted expression profiles. The highest brain concentrations of $\alpha$3 nAChR subunits are detected in the medial habenula (mHb), with much lower levels detected in the interpeduncular nucleus (IPn), superior cervical ganglion, superior colliculus, pineal gland, and the nucleus of the solitary tract (Wada et al., 1989; Sheffield et al., 2000; Yeh et al., 2001). Chrna5 knock-out mice, which do not express functional $\alpha$5* nAChRs, consume greater quantities of nicotine than their wild-type littermates, reflected by greater responding for the drug in the intravenous self-administration procedure (Fowler et al., 2011). Virus-mediated re-expression of $\alpha$5 nAChR subunits in the mHb-IPn circuit of Chrna5 knock-out mice normalizes their otherwise increased levels of nicotine intake (Fowler et al., 2011). Conversely, virus-mediated knock-down of $\alpha$5 subunits in the mHb-IPn circuit, transient inactivation of this pathway accomplished by local infusions of the anesthetic lidocaine, or pharmacological blockade of NMDA receptor-mediated glutamatergic transmission in the IPn, all result in increased nicotine intake in rats (Fowler et al., 2011). Furthermore, overexpression of $\beta$4 nAChR subunits increases the aversive properties of nicotine in mice, with this action thought to reflect enhanced sensitivity of mHb neurons to the stimulatory actions of nicotine (Frahm et al., 2011). Together, these findings suggest the mHb-IPn circuit regulates nicotine avoidance behaviors, which protect against risk of developing tobacco dependence (Fowler and Kenny, 2014). Considering their high concentrations in the mHb-IPn circuit, we tested the hypothesis that $\alpha$3* nAChRs located in this circuit regulate the motivational properties of nicotine.

## Materials and Methods

### Animals
Male and female C.129S(B6)-Chrna3$^{tm1.1Hwrt}$/J (Chrna3$^{tm1.1Hwrt}$) mice were obtained from The Jackson Laboratory and bred in our animal facilities with wild-type BALB/cJ mice. The mutant mice were maintained on this BALB/cJ background to enhance their rates of survival (<60% survival on BALB/c background versus <2% survival on C57BL/6 or 129S background; https://www.jax.org/strain/012621). Breeding was conducted by mating heterozygous pairs to obtain experimental subjects. All mice were at least six weeks of age at the time when experiments were initiated. Male Wistar rats (275–300 g) were obtained from Charles River and housed one to two per cage. Mice and rats were group housed (two to three per cage) and maintained in an environmentally controlled vivarium on a 12/12 h reversed light/dark cycle. During self-administration procedures, subjects were food restricted to 85–90% of their free-feeding body weight, with water available ad libitum. All procedures were conducted in strict accordance with the National Institutes of Health Guide for the Care and Use of Laboratory Animals and approved by the Institutional Animal Care and Use Committee.

### Genotyping
Around 21 d of age mouse pups were weaned, and their tails were clipped for genetic analysis. Genotyping was performed as previously described (Fowler et al., 2011). The primers used were as follows: forward (5′-TGT GTT GTC CCT GTC TGC TC-3′) and reverse (5′-GCA AGT CCC CTT AAT TGC TG-3′). The band for the wild-type gene was at 211 bp, and the $\alpha$3 mutant gene was ~320 bp.

### Drugs
For intravenous self-administration, (-)-nicotine hydrogen tartrate salt (Sigma) was dissolved in 0.9% sterile saline (pH ~7.4). All doses of nicotine refer to free-base. $\alpha$-Conotoxin AuIB, $\alpha$-conotoxin MII and mecamylamine were purchased from Tocris. Catheter integrity was tested using the ultrashort-acting barbiturate anesthetic Brevital (methohexital sodium, Eli Lilly).

### Generation of lentivirus
For $\alpha$3 subunit knock-down, short hairpin interfering RNAs (shRNA) directed against transcripts of the rat Chrna3 gene were designed using the GenScript online construct builder (shRNA sequence). The following sequence was used for all experiments: GCC ATG GTG ATT GAT CGC ATC). The shRNA was cloned into the pRNAT-U6.2/Lenti construct containing GFP (GenScript). The control vector was identical but without the gene insert. To generate lentivirus supernatant, HEK-293FT packaging cells ($3.75 \times 10$6,293 cells per 10-cm plate) were transfected with the vectors along with the pPACKF1TM Lentiviral Packaging kit using lipofectamine reagent and plus reagent (Invitrogen). Medium containing virus particles (~10 ml) was harvested 48–60 h posttransfection by centrifugation at $76,755 \times g$ for 5 min to pellet cell debris. Supernatant was filtered through 0.45-mm polyvinylidene difluoride (PVDF) filters (Millex-HV), centrifuged at $32,000 \times g$ for 90 min and the precipitate re-suspended in 100-$\mu$l PBS. Supernatants were aliquoted into 10-$\mu$l volumes and stored at −80°C until use. Viral supernatant titers were determined using the Lentivector Rapid Titer kit (System Biosciences). The number of infectious units per ml of supernatant (IFU ml$^{-1}$) was calculated as follows: multiplicity of infection (MOI) of the sample × the number of cells in the well on infection × 1000/$\mu$l of viral supernatant.

### RNA isolation and real-time RT-PCR
Rats were euthanized by inhalation of $CO_2$, their brains rapidly removed and frozen on dry ice, then stored at −80°C until use. Brains were sliced on a cryostat, and samples from mHb, IPn, and other sites were collected and pooled across subjects because of the small size of brain area, then stored at −80°C until RNA isolation. Cells grown in monolayer or dissected brain tissue was homogenized in RNA-STAT60 (Tel-Test Inc.) and vortexed with chloroform. Samples were centrifuged for 15 min at $12,000 \times g$ and the upper aqueous RNA-containing layer was removed for an additional RNASTAT60/chloroform extraction. The RNA was precipitated with isopropanol overnight at −20°C and centrifuged for 30 min at $12,000 \times g$. The RNA pellets were washed twice with 70% ethanol/RNAase-free water and subsequently resuspended in RNAsecure (Ambion/Applied Biosystems), and ~10 µg of RNA from each sample was treated with Turbo DNase (Ambion/Applied Biosystems) for 60 min at 37°C to degrade residual genomic DNA. To assess RNA levels, samples were reverse transcribed into cDNA using the TaqMan High Capacity cDNA Reverse Transcription kit (Applied Biosystems). They were then processed using the TaqMan Universal PCR kit and the rat Chrna3 gene expression assay (Applied Biosystems). Samples were quantified by real-time RT-PCR (7900 Real-Time PCR system; Applied Biosystems). All data were normalized to $\beta$-actin levels as an internal control. Comparison between groups were made using the method of $2^{-\Delta\Delta Ct}$.

### Intravenous surgery
Mice and rats were anesthetized using an isoflurane (1–3%)/oxygen vapor mixture and prepared with intravenous catheters. Catheters consisted of a 6-cm (mice) or 12-cm (rats) length of SILASTIC tubing fitted to guide cannula (Plastics One), which was bent at a curved right angle and encased in dental acrylic. The catheter tubing was passed subcutaneously from the animals back to the right jugular vein, and a 1-cm (mice) or 2.5-cm (rats) length of catheter tip inserted into the vein, then secured to the vein with surgical silk suture. Catheters were flushed daily with physiological sterile saline solution (0.9%, w/v) containing heparin (10–60 USP units/ml). Catheter integrity at the end of each experiment was tested using Brevital.

*Intracranial surgery*

For lentivirus microinjections, rats were anesthetized using an isoflurane (1–3%)/oxygen vapor mixture and positioned in a stereotaxic frame (Kopf Instruments). To target the mHb (bilateral), the incisor bar was adjusted to 5 mm above plane, and the injector needle was adjusted to a 10° angle toward midline (AP: −2.2 mm from bregma; ML: ±1.5 mm from midline; DV: −4.9 mm from brain surface). For the IPn, the incisor bar was adjusted to the flat skull position and the injector needle was angled at 10° toward midline (AP: −6.72 mm from bregma; ML: ±1.6 mm from midline; DV: −8.5 mm from brain surface). For conotoxin injections, rats were implanted with guide cannula (Plastics One) positioned 2 mm above the IPn (10° angle toward midline, AP: −6.72 mm from bregma; ML: ±1.6 mm from midline; DV: −6.5 mm from brain surface). The injector needle extended 2 mm below the tip of the cannula. All of the injections (1-µl injection volume) were administered at a rate of 1 µl per min; the injector needle was left in place for an additional 2 min after the injection to allow for diffusion. For conotoxin microinjections into the IPn, infusions occurred ~10 min before the initiation of the self-administration session.

*Intravenous self-administration*

Mice and rats were mildly food restricted to 85–90% of their free-feeding body weight and trained to press a lever in an operant chamber (Med Associates) for food pellets (20-mg pellets mice, 45-mg pellets rats; TestDiet) under a fixed-ratio 5, time out 20 s (FR5TO20) schedule of reinforcement. Once stable responding was established (~30 pellets per session in mice; ~90 pellets per session in rats), which required approximately five sessions in mice and rats, subjects were prepared with intravenous jugular catheters as described above. The animals were permitted ≥48 h to recover from surgery then permitted to acquire intravenous nicotine self-administration behavior by autoshaping during 1-h daily sessions, 6–7 d per week. Specifically, animals were placed into the operant chamber and permitted to respond on the previously food-reinforced lever according to the same FR5TO20 schedule of reinforcement until stable responding for nicotine infusions was established. Nicotine was delivered through silastic tubing connected at one end to the intravenous catheter and at the other to a Razel syringe pump (Med Associates). Each session was conducted using two retractable levers (one active, one inactive). Completion of the response criteria on the active lever resulted in the delivery of an intravenous nicotine infusion (0.03-ml infusion volume for mice; 0.1-ml volume for rats). Responses on the inactive lever were recorded but had no scheduled consequences. The animals were presented with each dose of nicotine for at least 3 d, and the mean intake for the last two sessions was used for statistical analyses. For rats, nicotine doses were presented according to a within-subject Latin square design. Between each dose, subjects were permitted to respond for the training dose of nicotine (0.1 mg kg$^{-1}$ per infusion for mice; 0.03 mg kg$^{-1}$ per infusion for rats) for 2 d or until responding returned to baseline levels. For mice, nicotine doses were presented according to an ascending dose schedule (0.03 then 0.4 g kg$^{-1}$ per infusion) before mice were permitted to respond for saline. Subjects were excluded from analyses if catheter integrity was compromised during the experiment (visual leakage) or they failed to respond to intravenous Brevital infusion delivered after the final self-administration session had been completed.

*Fluorescence immunolabeling*

Subjects were anesthetized with a ketamine (100 mg kg$^{-1}$)/xylazine (10 mg kg$^{-1}$) drug combination and perfused through the ascending aorta with 0.9% saline, followed by 4% paraformaldehyde in 0.1 M PBS (pH 7.4). Brains were harvested, postfixed for 2 h, and then stored in 30% sucrose in PBS. All brains were cut into 40-µm coronal sections on a cryostat, and sections stored in 0.1 M PBS with 0.01% sodium azide at 4°C. To determine the location of lentivirus-infected cells (tagged with GFP), we used a chicken polyclonal IgG that recognizes a 27-kDa protein derived from the jellyfish *Aequorea victoria*. To identify IPn, we used a guinea pig polyclonal IgG that recognizes the vesicular ACh transporter (VAChT). Sections were rinsed in 0.1 M PBS with 0.3% Triton X-100 (PBT) and then blocked in 10% normal donkey serum/

PBT. Thereafter, sections were incubated in the primary antibody, chicken anti-GFP (1:2000; Millipore) or guinea pig anti-VAChT (1:500; Millipore), in PBT at 4°C overnight. The sections were rinsed and incubated in DyLight 488 donkey anti-chicken (1:400; Jackson ImmunoResearch) and/or DyLight 594 donkey anti-guinea pig (1:400; Jackson ImmunoResearch) in 0.3% PBT for 2 h. Finally, the sections were rinsed, mounted on slides with vectashield containing DAPI (Vector Laboratories), and coverslipped. Control procedures included processing the secondary antibodies alone to verify background staining, processing each primary with the secondary antibody to verify laser-specific excitation, assessing autofluorescence in an alternate laser channel with tissue lacking that laser-specific probe, and using sequential scanning. For subsequent fluorescent images, only the brightness and/or contrast levels were adjusted postacquisition and were imposed across the entire image.

*Brain slice preparation for electrophysiology recordings*

Male rats (three to six months) were used for all electrophysiology experiments. Rats were anesthetized with isoflurane followed by transcardial perfusion with oxygenated (95% O$_2$/5% CO$_2$) NMDG HEPES solution (92 mM NMDG, 2.5 mM KCl, 1.2 mM NaH$_2$PO$_4$, 30 mM NaHCO$_3$, 20 mM HEPES, 25 mM glucose, 5 mM Na$^+$ ascorbate, 2 mM thiourea, 3 mM Na$^+$ pyruvate, 10 mM MgSO$_4$ 7H$_2$O, 0.5 mM CaCl$_2$, and 2 mM H$_2$O, with pH adjusted to 7.3–7.4, 300–310 mOsm). The brain was quickly removed into ice-cold NMDG HEPES solution for >1 min; 300-µm-thick coronal slices containing mHb were cut using a vibratome (Leica VT1200S). Slices were then moved into a prewarmed (32°C) recovery chamber and conducted the stepwise Na$^+$ spike-in procedure (Ting et al., 2018), then kept at room temperature for at least 1 h, in the following solution: 95% O$_2$/5% CO$_2$-equilibrated HEPES-holding-solution containing the following: 92 mM NaCl, 2.5 mM KCl, 1.2 mM NaH$_2$PO$_4$, 30 mM NaHCO$_3$, 20 mM HEPES, 25 mM glucose, 5 mM Na$^+$ ascorbate, 2 mM thiourea, 3 mM Na$^+$ pyruvate, 2 mM MgSO$_4$ 7H$_2$O, and 2 mM CaCl$_2$ 2H$_2$O.

*Effects of α3\* nAChR-selective antagonists on nicotine-evoked currents*

Recordings were made under an upright microscope (Scientifica SliceScope Pro 2000, Scientifica) equipped with infrared differential interference contrast optics for visualization. Slices were transferred to a recording chamber and superfused with standard recording artificial CSF (aCSF) containing the following: 124 mM NaCl, 2.5 mM KCl, 1.2 mM NaH$_2$PO$_4$, 24 mM NaHCO$_3$, 5 mM HEPES, 12.5 mM glucose, 2 mM MgSO$_4$ 7H$_2$O and 2 mM CaCl$_2$ 2H$_2$O, adjusted to pH 7.3–7.4, 295–305 mOsm. All data were recorded from the soma of mHb neurons at 32°C using a Multiclamp 700B amplifier (Molecular Devices), filtered at 3 kHz, amplified five times, and then digitized at 10 kHz with a Digidata 1550 analog-to-digital converter (Molecular Devices). Input resistance was monitored continuously, and data from experiments were discarded if this parameter changed by >20% during recordings. Patch pipettes were made from borosilicate glass capillary tubing (1B150F-4; World Precision Instruments) using a micropipette puller (PC-10; Narishige). To isolate nAChR currents, the internal recording pipette solution was potassium-based and contained the following: 130 mM K$^+$ gluconate, 4 mM KCl, 0.3 mM EGTA, 10 mM HEPES, 4 mM MgATP, 0.3 mM Na$_2$GTP, and 10 mM phosphocreatine; pH adjusted to 7.3 with KOH while the external solution was aCSF +0.5 µM TTX+ 100 µM picrotoxin, + 5 µM NBQX+ 50 µM APV. Voltage was held at −60 mV (Vhold = −60 mV). For nicotine application, a glass pipette filled with nicotine solution (30 µM), identical to a typical recording pipette, was connected to a micropressure ejection system (PICOSPRTIZER®III, Parker, USA). Ejection pipettes were moved to ~20–40 µm of the recorded cell using a manipulator and nicotine applied every 60 s. A baseline nAChR current was recorded for 5 min, then vehicle (aCSF) or each concentration of nAChR antagonist was applied using the same perfusion system by switching the perfusion line.

*Statistical analyses*

All data were analyzed by two-tailed *t* test or by one-way or two-way ANOVA using within-subject or between-subject comparisons with or

without repeated measures, as appropriate. Analyses were conducted using GraphPad Prism software. Statistically significant main or interaction effects were followed by Bonferroni *post hoc* tests. The criterion for statistical significance was set at $p < 0.05$.

## Results

$Chrna3^{tm1.1Hwrt}$ mice had reduced body weights and were smaller in size compared with their wild-type littermates (Fig. 1A), consistent with reports from the vendor. When we trained adult male and female $Chrna^{3tm1.1Hwrt}$ mice ($n = 12$ in total) to lever-press for food rewards under a FR5TO20 schedule of reinforcement, they demonstrated no overt behavioral abnormalities and earned similar numbers of food pellets as male and female wild-type mice ($n = 12$; two-way ANOVA: genotype × session interaction: $F_{(5,100)} = 0.699$, $p = 0.6255$; data from sessions 5–10 after stable responding was established; Fig. 1B). When the mice were permitted to respond for intravenous nicotine infusions, we found that $Chrna3^{tm1.1Hwrt}$ mice tolerated the drug poorly and showed a high level of post-session sickness or death in response to nicotine consumption. Of the original 12 $Chrna3^{tm1.1Hwrt}$ mice, five males and four females were euthanized or found dead during the nicotine self-administration phase of the experiment, with only three female mutant mice completing the entire experiment (Fig. 1C). By contrast, only a single female wild-type mouse became ill and was euthanized over the course of the entire experiment (Fisher's exact test: $p = 0.001$; Fig. 1C). When we compared nicotine responding data collected from the surviving $Chrna3^{tm1.1Hwrt}$ mice with data collected from the 5 female wild-type littermates, we found that the mutant mice responded at higher levels for nicotine (two-way ANOVA: genotype: $F_{(1,6)} = 11.62$, $p = 0.0358$; dose: $F_{(2,12)} = 28.89$, $p < 0.0001$; interaction: $F_{(2,12)} = 4.985$, $p = 0.0266$; Fig. 1D). Analysis of the absolute amounts of nicotine consumed at each unit dose of the drug (number of infusions earned × unit dose of nicotine) showed that intake differed between $Chrna3^{tm1.1Hwrt}$ mice and wild-type mice (two-way ANOVA: genotype: $F_{(1,6)} = 11.62$, $p < 0.05$; dose: $F_{(2,12)} = 51.8$, $p < 0.0001$; interaction: $F_{(2,12)} = 21.7$, $p = 0.0001$; Fig. 1E). This effect was evident at the 0.4 mg kg$^{-1}$ unit dose, at which the mutant mice self-administered around four times more nicotine than wild-type mice (Fig. 1E).

Next, we investigated the role for α3* nAChRs in the mHb-IPn circuit in regulating nicotine intake. To accomplish this, we generated a shRNA directed against rat *Chrna3* gene transcripts (Lenti-shRNA-*Chrna3*) to knock-down α3 subunit expression (Fig. 2A). To control for the effects of virus transduction, a second lentivirus was developed that was identical to Lenti-shRNA-*Chrna3* but did not contain the shRNA insert (Lenti-Control). We packaged the vectors into lentivirus particles and confirmed that they efficiently transduced mHb neurons *in vivo* (Fig. 2B). Indeed, we detected cells expressing green-fluorescent protein (GFP$^+$) in the mHb but not in surrounding brain sites of rats after microinjection of Lenti-shRNA-*Chrna3* into the mHb (Fig. 2B). GFP$^+$ axons were also detected in the IPn (Fig. 2B), the main site to which mHb neurons project. We also confirmed that Lenti-shRNA-*Chrna3* knocked down *Chrna3* transcript expression. Using real-time PCR (RT-PCR), we found that α3



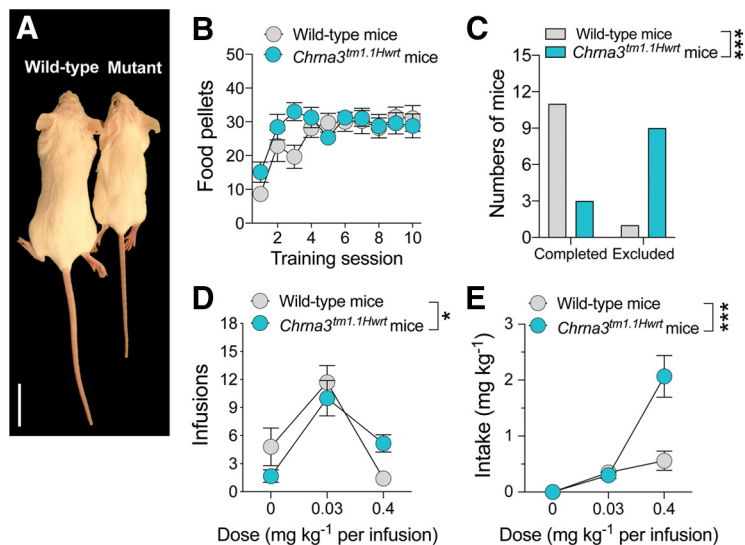**Figure 1.** Increased nicotine intake in mice with hypomorphic α3 nAChR subunit expression. ***A***, Representative image demonstrating gross size difference between wild-type mice (left) and $Chrna3^{tm1.1Hwrt}$ mutant littermates (right). Scale bar: 2 cm. ***B***, Acquisition of food responding (20-mg pellets) in $Chrna3^{tm1.1Hwrt}$ mutant mice ($n = 5$ males; $n = 6$ females) and wild-type littermates ($n = 6$ males; $n = 6$ females). Data are presented as mean (±SEM) number of food rewards earned. ***C***, Numbers of $Chrna3^{tm1.1Hwrt}$ mutant mice and wild-type littermates that completed the nicotine self-administration phase of the experiment and numbers that were excluded because of nicotine-induced illness or death; ∗∗∗$p = 0.001$, Fisher's exact test. ***D***, Nicotine self-administration behavior when different unit doses of nicotine were available in the mutant female ($n = 3$) and wild-type ($n = 5$) mice that completed the study. Data are presented as mean (±SEM) number of nicotine infusions; ∗$p < 0.01$, main effect of genotype in two-way repeated-measures ANOVA. ***E***, Total quantities of nicotine consumed for each unit doses that was available in the mutant female ($n = 3$) and wild-type ($n = 5$) mice that completed the study. Data are presented as mean (±SEM) total nicotine intake; ∗∗∗$p < 0.001$, main effect of genotype in two-way repeated-measures ANOVA.

subunit mRNA expression was lower in rat PC12 cells, which constitutively express *Chrna3* transcripts, after transfection with Lenti-shRNA-*Chrna3* compared with the Lenti-Control construct ($t_{(4)} = 55.35$, $p < 0.0001$; Fig. 2C). Similarly, α3 subunit transcripts were reduced (~70%) in habenular tissue collected from rats approximately three weeks after they were microinjected into the mHb with Lenti-shRNA-*Chrna3* particles compared with rats injected with Lenti-Control particles ($t_{(2)} = 3.498$, $p < 0.05$; Fig. 2D). Hence, the Lenti-shRNA-*Chrna3* vector efficiently transduces mHb neurons and knocks down α3 nAChR subunit expression.

Next, to investigate the effects of knocking down α3 nAChR subunit expression in mHb neurons on the reinforcing properties of nicotine, rats were injected with Lenti-shRNA-*Chrna3* or Lenti-Control vectors into the mHb. Approximately three weeks later, both groups of virus-treated rats were trained to lever-press for food rewards during 1 h daily sessions until they established stable responding under a FR5TO20 schedule of reinforcement. The Lenti-shRNA-*Chrna3* and Lenti-Control rats did not differ in their acquisition of the lever-press response and earned similar numbers of food rewards (two-way ANOVA: lentivirus × session interaction: $F_{(5,195)} = 0.441$, $p = 0.819$; data not shown). Rats were then implanted with jugular catheters and permitted to respond for intravenous nicotine infusions (0.03 mg kg$^{-1}$ per infusion) for at least 7 d under a FR5TO20 schedule of reinforcement until stable intake was established. The Lenti-shRNA-*Chrna3* and Lenti-Control rats did not differ in the number of nicotine infusions they earned, with both groups demonstrating stable levels of responding after approximately five sessions (two-way ANOVA: lentivirus × session interaction: $F_{(7,228)} = 1.161$, $p = 0.328$; data not shown). Thereafter, the unit dose of
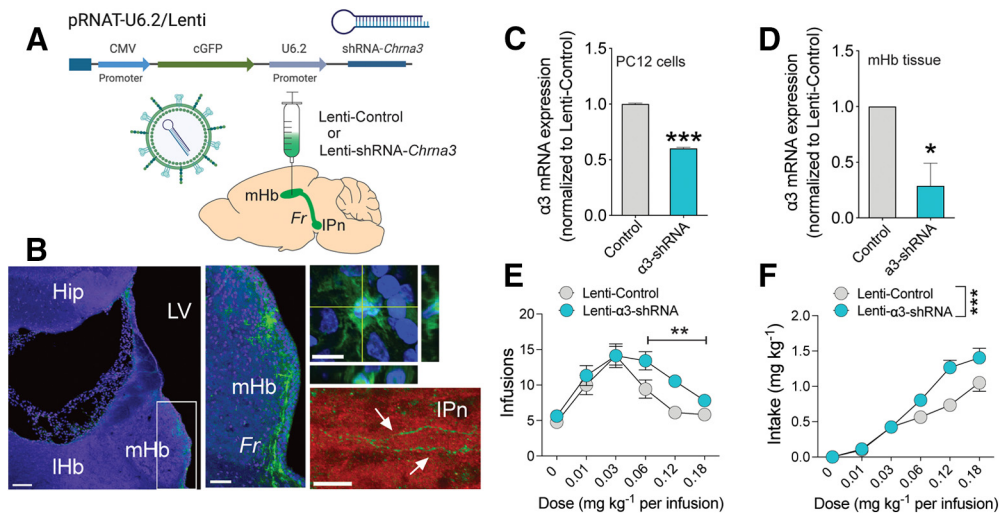
**Figure 2.** Lentiviral-mediated knock-down of the α3 nAChR subunit. **A**, Map of pRNAT-U6.2/Lenti vector used to generate Lenti-shRNA-*Chrna3* and Lenti-Control viruses. Also shown is a graphical representation of the microinjection of lentivirus particles into mHb of rats. **B**, Immunostaining for GFP (green) confirms lentivirus-infected cells were localized to the mHb (left panel). The tissue is counterstained with DAPI (blue). Hip, hippocampus; lHb, lateral habenula; LV, lateral ventricle; mHb, medial habenula; Fr, fasciculus retroflexus. Scale bar: 100 μm. Also shown is a higher-magnification image of GFP-expressing cells in the area outlined by the white box (middle panel). Fr, fasciculus retroflexus. Scale bar: 50 μm. The upper right panel shows an image of a GFP and DAPI co-labeled cell in the mHb. The cross-marks indicate the location of the smaller panel views along the y-z-axis (right) and x-z-axis (below) to demonstrate 3D localization of GFP and DAPI. Scale bar: 10 μm. The lower right panel shows an image of GFP-labeled axons (arrows) in the IPn. VAChT-labeling (red) demonstrates specificity of expression in IPn. Scale bar: 50 μm. **C**, Real-time PCR data for α3 subunit mRNA in PC12 cells 24 h posttransfection with the Lenti-shRNA-*Chrna3* vector. Data are presented as mean (±SEM) fold change compared with the control mean (method of $2^{-\Delta\Delta Ct}$); $***p < 0.0001$, unpaired $t$ test. **D**, Real-time PCR data for α3 subunit mRNA in habenular tissue of rats approximately three weeks after microinjection of Lenti-Control or Lenti-shRNA-*Chrna3* particles into the mHb. Data are presented as mean (±SEM) fold change; $*p < 0.05$, unpaired $t$ test. **E**, Nicotine responding in male rats expressing Lenti-Control ($n = 24$) or Lenti-shRNA-*Chrna3* ($n = 16$) in the mHb across a broad range of nicotine doses. Data are presented as mean (±SEM) number of nicotine infusions; $**p < 0.01$, main effect of virus in two-way repeated-measures ANOVA for unit doses 0.06–0.18 mg kg$^{-1}$. **F**, Quantities of nicotine consumed at each unit dose available were calculated. Data are presented as mean (±SEM) total nicotine intake; $***p < 0.001$, main effect of virus in two-way repeated-measures ANOVA.
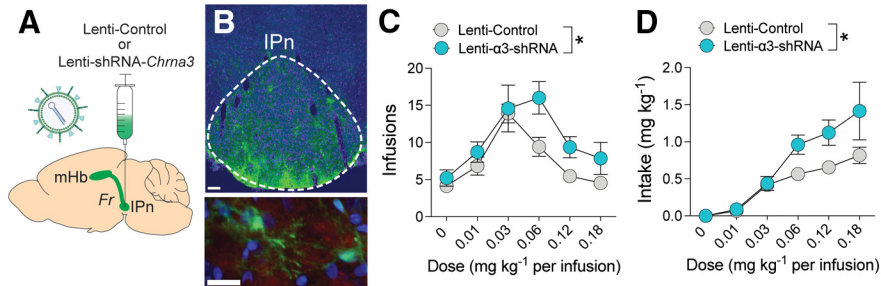


**Figure 3.** Knock-down of α3 nAChR subunit expression in the IPn increases nicotine intake in rats. **A**, Graphical representation of the microinjection of Lenti-Control or Lenti-shRNA-*Chrna3* particles into IPn of rats. **B**, The upper panel shows a representative image of GFP-labeling (green) in the IPn with DAPI counterstaining (blue). Scale bar: 100 μm. Lower panel shows a higher-magnification image of GFP (green) and DAPI (blue) colocalized labeling in cells in the IPn. Section is counterstained with VCHAT (red) to confirm localization of GFP-positive cells specifically in the IPn. Scale bar: 10 μm. **C**, Nicotine self-administration in male rats expressing Lenti-Control ($n = 11$) or Lenti-shRNA-*Chrna3* ($n = 7$) in the IPn across a broad range of doses. Data are presented as mean (±SEM) number of nicotine infusions; $*p < 0.05$, main effect of virus in two-way repeated-measures ANOVA. **D**, The total quantities of nicotine consumed at each unit dose available were calculated. Data are presented as mean (±SEM) total nicotine intake; $*p < 0.05$, main effect of virus in two-way repeated-measures ANOVA.

nicotine available for self-administration was varied to generate a dose–response function. The Lenti-shRNA-*Chrna3* rats tended to respond at higher levels than Lenti-Control rats for nicotine infusions, with this effect most apparent for doses on the descending portion of the dose–response function (two-way ANOVA: lentivirus: $F_{(1,38)} = 3.766$, $p = 0.0598$; dose: $F_{(5,190)} = 20.67$, $p < 0.0001$; interaction: $F_{(5,190)} = 1.409$, $p = 0.22$; Fig. 2E). Previously, we found that shRNA-mediated knock-down of *Chrna5* transcripts in mHb increased nicotine self-administration in rats only for unit doses on the descending portion of the dose-response function ($>0.06$ mg kg$^{-1}$; Fowler et al., 2011). Therefore, we compared responding between groups for the

higher unit doses of nicotine (0.06–0.18 mg kg$^{-1}$). At these doses, responding was higher in Lenti-shRNA-*Chrna3* rats compared with Lenti-Control rats (Fig. 2E; two-way ANOVA: lentivirus: $F_{(1,38)} = 9.93$, $p = 0.0032$; dose: $F_{(2,76)} = 10.68$, $p < 0.0001$; interaction: $F_{(2,76)} = 1.527$, $p = 0.2237$). When total quantities of nicotine consumed at each unit dose were calculated, we found that Lenti-shRNA-*Chrna3* rats consumed greater quantities than Lenti-Control rats (two-way ANOVA: lentivirus: $F_{(1,38)} = 8.780$, $p = 0.0052$; dose: $F_{(5,190)} = 109.9$, $p < 0.0001$; interaction: $F_{(5,190)} = 6.604$, $p < 0.0001$; Fig. 2F).

To investigate whether α3∗ nAChRs in the IPn regulate nicotine intake, we injected Lenti-shRNA-*Chrna3* or Lenti-Control vectors into the IPn of rats (Fig. 3A). Approximately three to four weeks later, GFP$^+$ cells were detected within the IPn and not in surrounding brain sites (Fig. 3B). Rats injected with Lenti-shRNA-*Chrna3* did not differ from Lenti-Control rats in their responding for food rewards under the FR5TO20 schedule (two-way ANOVA: lentivirus: $F_{(1,16)} = 1.291$, $p = 0.273$; session: $F_{(5,80)} = 55.85$, $p < 0.0001$; interaction: $F_{(5,80)} = 2.054$, $p = 0.08$; data not shown). Similarly, responding for the training dose of 0.03 mg kg$^{-1}$ per infusion did not differ between the groups, with both groups demonstrating stable levels of responding after approximately five sessions (two-way ANOVA: lentivirus: $F_{(1,16)} = 1.129$, $p = 0.886$; session: $F_{(7,112)} = 8.785$, $p = 0.0002$; interaction: $F_{(7,112)} = 0.886$, $p = 0.521$; data not shown). After
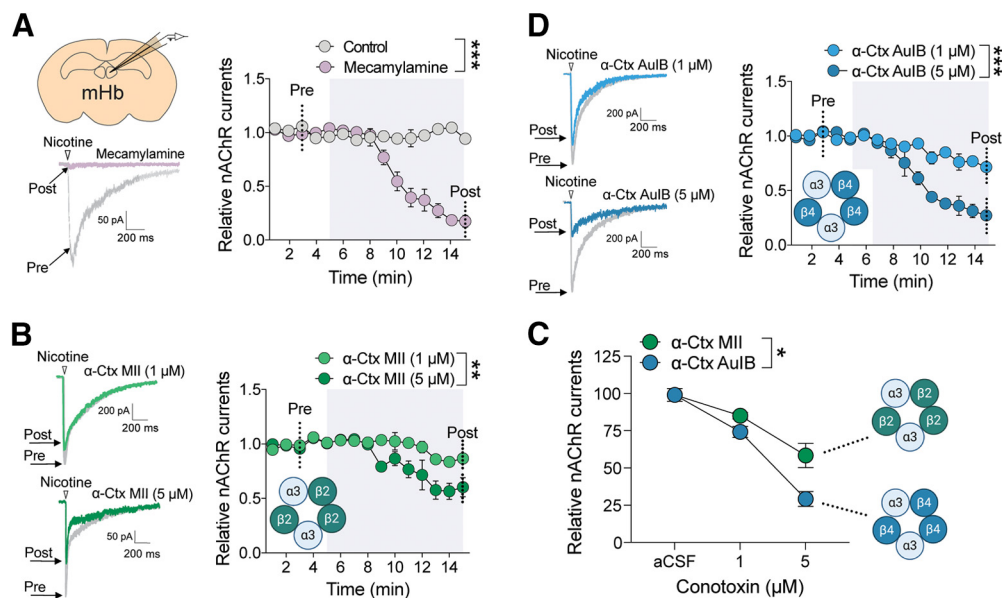
**Figure 4.** $\alpha3\beta4$ nAChRs regulate the stimulatory effects of nicotine on mHb neurons. ***A***, Graphical representation of the whole-cell recording procedure used to measure the stimulatory effects of nicotine on mHb neurons (upper panel) and representative nAChR current traces in mHb neurons evoked by nicotine (30 $\mu$M) pulses (every 60 s) before and after treatment with mecamylamine (10 $\mu$M; lower panel). Also shown is the mean relative nAChR-mediated currents ($\pm$SEM) in mHb neurons superfused (shaded area) with aCSF ($n = 3$ cells from $n = 3$ rats) or mecamylamine (10 $\mu$M; $n = 4$ cells/$n = 4$ rats); ∗∗∗$p < 0.001$, main effect of mecamylamine in two-way repeated-measures ANOVA. ***B***, Representative nAChR current traces in mHb neurons before and after treatment with $\alpha$-conotoxin MII ($\alpha$-Ctx MII; 1 or 5 $\mu$M; left panel). Mean relative nAChR-mediated currents ($\pm$SEM) in mHb neurons superfused (shaded area) with $\alpha$-Ctx MII (1 $\mu$M, $n = 5$ cells/$n = 5$ rats or 5 $\mu$M, $n = 3$ cells/$n = 3$ rats; right panel); ∗∗$p < 0.01$, main effect of concentration in two-way repeated-measures ANOVA. ***C***, Representative nAChR current traces in mHb neurons before and after treatment with $\alpha$-conotoxin AuIB ($\alpha$-Ctx AuIB; 1 or 5 $\mu$M; left panel). Mean relative nAChR-mediated currents ($\pm$SEM) in mHb neurons superfused (shaded area) with $\alpha$-Ctx MII (1 $\mu$M, $n = 5$ cells/$n = 5$ rats or 5 $\mu$M, $n = 3$ cells/$n = 3$ rats; right panel); ∗∗∗$p < 0.001$, main effect of concentration in two-way repeated-measures ANOVA. ***D***, Mean relative nAChR-mediated currents ($\pm$SEM) in mHb neurons treated with $\alpha$-Ctx MII or $\alpha$-Ctx AuIB; ∗$p < 0.05$, interaction effect in two-way repeated-measures ANOVA.

stable responding was established at the training dose, both groups were permitted to respond for a range of nicotine doses as described above. We found that Lenti-shRNA-*Chrna3* rats responded more vigorously than Lenti-Control rats (two-way ANOVA: lentivirus: $F_{(1,16)} = 6.165$, $p = 0.0245$; dose: $F_{(5,80)} = 17.22$, $p < 0.0001$; interaction: $F_{(5,80)} = 1.45$, $p = 0.2155$; Fig. 3C). When total quantities of nicotine consumed for each unit dose were calculated, we found the Lenti-shRNA-*Chrna3* rats consumed significantly greater quantities of nicotine than Lenti-Control rats (two-way ANOVA: lentivirus: $F_{(1,16)} = 8.146$, $p < 0.05$; dose: $F_{(5,80)} = 34.15$, $p < 0.0001$; interaction: $F_{(5,80)} = 2.989$, $p < 0.05$; Fig. 3D).

$\alpha3$ nAChR subunits can combine with $\beta2$ or $\beta4$ subunits to form functional $\alpha3\beta2*$ or $\alpha3\beta4*$ nAChRs, respectively. We used whole-cell recordings to investigate whether either or both of these $\alpha3*$ nAChR subtypes regulate the stimulatory effects of nicotine on the mHb-IPn circuit (Fig. 4A). First, we confirmed that nicotine-evoked nAChR-mediated currents in mHb neurons can be pharmacologically isolated. The relatively non-selective but $\alpha3*$ nAChR preferring nAChR antagonist mecamylamine (10 $\mu$M) abolished pharmacologically isolated currents evoked by nicotine in mHb neurons (>80% inhibition), confirming that these currents were regulated by nAChRs (two-way ANOVA: mecamylamine: $F_{(1,5)} = 35.63$; $p = 0.01$; incubation time: $F_{(14,70)} = 32.12$, $p < 0.0001$; interaction: $F_{(14,70)} = 32.48$, $p < 0.0001$; Fig. 4A). The $\alpha3\beta2*$ nAChR antagonist $\alpha$-conotoxin MII (1–5 $\mu$M) attenuated nicotine-evoked currents in mHb neurons (~40% maximum inhibition; two-way ANOVA: concentration: $F_{(1,6)} = 19.06$; $p = 0.0047$; incubation time: $F_{(14,84)} = 15.00$, $p < 0.0001$; interaction: $F_{(14,84)} = 4.449$, $p < 0.0001$; Fig. 4B). The $\alpha3\beta4*$ nAChR antagonist $\alpha$-conotoxin AuIB (1–5 $\mu$M) greatly attenuated nicotine-evoked currents in mHb neurons, with the highest

concentration almost completely abolishing the actions of nicotine (>70% inhibition; two-way ANOVA: concentration: $F_{(1,6)} = 39.31$; $p = 0.008$; incubation time: $F_{(14,84)} = 47.13$, $p < 0.0001$; interaction: $F_{(14,84)} = 12.07$, $p < 0.0001$; Fig. 4C). Direct comparison of the effects of $\alpha$-conotoxin MII and $\alpha$-conotoxin AuIB confirmed that $\alpha$-conotoxin AuIB had greater efficacy in blocking nicotine-evoked currents in mHb neurons (two-way ANOVA: conotoxin: $F_{(1,16)} = 13.03$, $p = 0.005$; concentration: $F_{(2,16)} = 66.95$, $p < 0.0001$; interaction: $F_{(2,16)} = 66.95$, $p < 0.0001$; Fig. 4D).

Finally, we investigated whether $\alpha3\beta2$ or $\alpha3\beta4$ nAChRs in the mHb-IPn circuit regulate nicotine intake. Rats surgically implanted with a guide cannula targeted toward the IPn were trained to intravenously self-administer nicotine (Fig. 5A). After stable levels of responding were established, rats received intra-IPn infusions of vehicle and $\alpha$-conotoxin AuIB (10 $\mu$M), or vehicle and $\alpha$-conotoxin MII (10 $\mu$M) according to a within-subject crossover designs. IPn infusion of $\alpha$-conotoxin MII had no effects on intake ($t_{(7)} = 0.102$, $p = 0.912$; Fig. 4B). By contrast, IPn infusion of $\alpha$-conotoxin AuIB increased nicotine intake ($t_{(8)} = 5.16$, $p < 0.001$; Fig. 5C). Accuracy of injection sites in IPn was confirmed for all rats included in the analyses (Fig. 5D).

## Discussion

Allelic variation in *CHRNA3*, the gene encoding the $\alpha3$ nAChR subunit, increases vulnerability to tobacco dependence in humans (Amos et al., 2008; Berrettini et al., 2008; Marques-Vidal et al., 2011; Ware et al., 2011). $\alpha3*$ nAChRs are densely expressed in the habenula-IPn circuit, which is known to regulate nicotine avoidance behaviors (Fowler et al., 2011; Frahm et al., 2011; Tuesta et al., 2017). Here, we show that mutant mice with hypomorphic expression of $\alpha3*$ nAChRs consume more
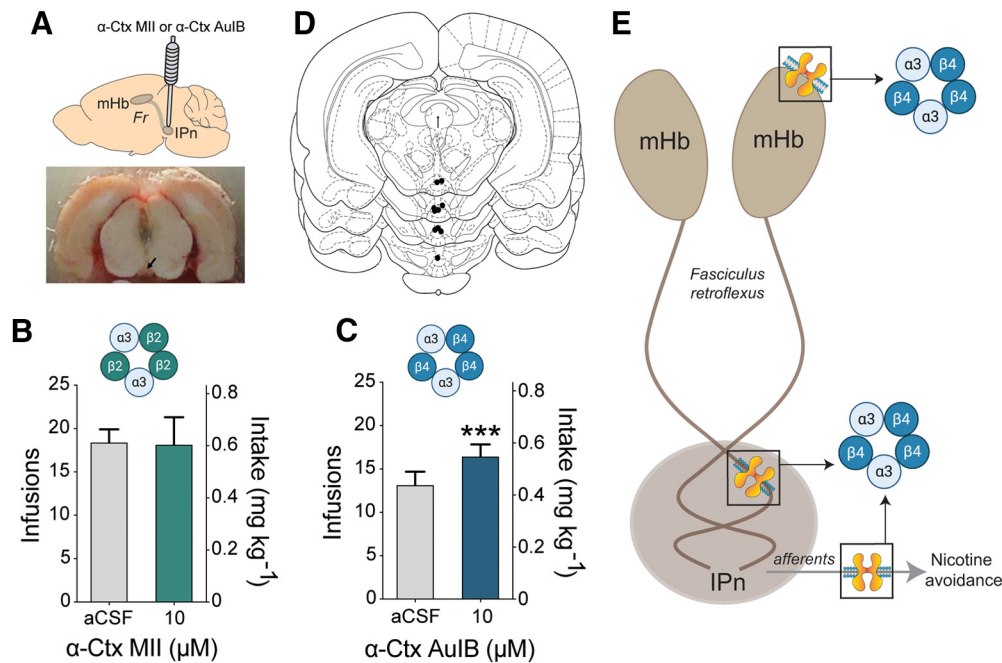
**Figure 5.** Infusion of α3β4-selective nAChR antagonist into IPn increases nicotine intake. **A,** Graphical representation of the microinjection of conotoxin into the IPn of rats (top panel). Also shown is a representative image of a coronal section highlighting the microinfusion site in the IPn of a rat (bottom panel). **B,** Nicotine self-administration in male rats (n = 8) injected with α-conotoxin MII or vehicle 10 min before the self-administration session. Data are presented as mean (± SEM) number of nicotine infusions. **C,** Nicotine self-administration in male rats (n = 9) injected with α-conotoxin AuIB or vehicle 10 min before the self-administration session according to a crossover design. Data are presented as mean (± SEM) number of nicotine infusions; ∗∗∗$p < 0.001$, paired $t$ test. **D,** Diagrammatic representation of coronal sections from the rat brain showing histologic reconstruction of the microinjection sites in the IPn. Black circles indicate locations of injector tips located inside the IPn from rats included in statistical analyses. **E,** Graphical summary of proposed mechanisms by which α3∗ nAChRs in the mHb-IPn circuit regulate nicotine intake. It is proposed that α3β4 nAChRs located somato-dendritically and presynaptically on mHb neurons, and on afferents from IPn neurons, are activated by nicotine to trigger nicotine avoidance behaviors.

nicotine than their wild-type littermates. Using an RNA interference approach, we found that knock-down of α3 nAChR subunit transcripts in the mHb or IPn increased nicotine intake in rats. Using slice electrophysiology recordings in rats, we show that α3β4 nAChRs play a prominent role in regulating the stimulatory effects of nicotine on mHb neurons. Finally, infusion of the α3β4 nAChR-selective antagonist α-conotoxin AuIB into the IPn of rats, the brain site to which mHb neurons project almost exclusively, increased nicotine intake in rats. These findings suggest that α3∗ nAChRs in the habenula-IPn circuit regulate nicotine intake (Fig. 5E). Hence, diminished α3∗ nAChR-mediated neurotransmission in the habenula-IPn circuit in individuals who carry *CHRNA3* risk alleles may contribute to their elevated levels of tobacco consumption and higher incidence of smoking-related diseases.

The α3 subunit was the first mammalian nAChR subunit to be cloned (Boulter et al., 1986), yet little is known about its role in the addiction-relevant behavioral actions of nicotine. A major obstacle has been the fact that null mutation of *Chrna3* results in postnatal lethality in mice (Xu et al., 1999). Recently, a mouse line with hypomorphic expression of α3 subunits was developed (Caffery et al., 2009). In these mice, the *Chrna3* gene was modified by introducing five nucleotide mutations in exon 5 and a loxP-flanked neomycin (neo) resistance cassette upstream of exon 5 (*Chrna3^{3tm1.1Hwrt}* mice; Caffery et al., 2009). These modifications result in reduced constitutive expression of α3∗ nAChRs (Caffery et al., 2009), and when maintained on a BALB/c background ~60% of the mutant mice survive to adulthood (Caffery et al., 2009). We observed no overt behavioral abnormalities in the *Chrna3^{3tm1.1Hwrt}* mice, and they learned to respond for food rewards in a manner indistinguishable from their wild-type littermates. By contrast, the mutant mice had elevated levels of

responding for intravenous nicotine infusions and consumed greater quantities of the drug. However, the *Chrna3^{3tm1.1Hwrt}* mice were remarkably sensitive to adverse effects of nicotine and showed sickness-like behavior after each self-administration session, with only three females but no male mutant mice successfully completing the experiment. This is consistent with the autonomic dysfunction previously reported in these mice (Caffery et al., 2009), and in mice with complete genetic ablation of the *Chrna3* gene (Xu et al., 1999), which was likely exacerbated by nicotine consumption. Although nicotine had such detrimental effects in the mutant mice, they persisted in responding for the drug and consumed greater quantities than their wild-type littermates. This continued consumption despite adverse outcomes is reminiscent of the compulsive tobacco use seen in habitual smokers that often persists despite awareness of potentially devastating health consequences. Such adverse responses to nicotine in the mutant mice, resulting in just a small number of females that successfully completed the entire experiment, raises notable concerns about their utility for addiction-focused behavioral studies. Nevertheless, these findings support a role for α3∗ nAChRs in regulating the motivational properties of nicotine. Moreover, these findings may have relevance to smoking-related diseases associated with autonomic dysfunction, such as cardiovascular disease or type-2 diabetes (Duncan et al., 2019; Garcia et al., 2020), in smokers who carry *CHRNA3* risk alleles that result in deficient α3∗ nAChR-mediated transmission.

The highest concentrations of α3∗ nAChRs in the mammalian brain are found in the habenula (Rassadi et al., 2005), with *Chrna3* transcripts also detected in the IPn (Rassadi et al., 2005; Caffery et al., 2009). To investigate whether α3∗ nAChRs in the habenula-IPn circuit regulate nicotine intake we developed a

lentivirus-based shRNA against *Chrna3* transcripts. Using this virus, we found that α3 subunit knock-down in the mHb or IPn of rats increased their nicotine intake. This finding is similar to the effects of knocking down α5 nAChR transcripts in the mHb in rats (Fowler et al., 2011). Conversely, overexpression of β4 subunits in the habenula-IPn circuit decreases nicotine intake in mice (Frahm et al., 2011). Hence, nAChRs that contain subunits encoded by the *CHRNA5/CHRNA3/CHRNB4* gene cluster, which has been heavily implicated in tobacco dependence vulnerability (Hung et al., 2008; Thorgeirsson et al., 2008), are likely to act in the habenula-IPn circuit to regulate nicotine intake. While disruption of α3∗ nAChR-mediated transmission, either globally in *Chrna3* hypomorphic mice or restricted to the habenula-IPn circuit in lentivirus- rats, increased nicotine intake, the effect sizes were relatively modest when compared with previous manipulations of *Chrna5* or other gene transcripts in this circuit performed by our group (Fowler et al., 2011; Tuesta et al., 2017; Duncan et al., 2019). This may suggest that while α3∗ nAChRs are involved in regulating the actions of nicotine on the habenula-IPn circuit, other nAChRs subtypes, most notably α4β2α5∗ nAChRs, may play a more prominent role. It is also noteworthy that α3∗ nAChR subunit knock-down in habenula or IPn did not impact the acquisition of nicotine self-administration in rats. However, the major smoking-related phenotype observed in those who carry *CHRNA3* risk alleles is a greater number of cigarettes smoked per day. This is thought to reflect the reduced aversive properties of nicotine in smokers who carry *CHRNA3/A5/B4* risk alleles (Jensen et al., 2015), which may in turn relate to attenuated actions of nicotine on the habenula-IPn circuit (Fowler et al., 2011). Consequently, abnormalities in rates of acquisition of nicotine self-administration behavior in α3 nAChR-deficient animals may be apparent only when unit doses of nicotine greater than $0.03 \text{ mg kg}^{-1}$ are used, which have greater stimulatory effects on the habenula-IPn circuit (Kenny and Markou, 2006; Kenny et al., 2009; Duncan et al., 2019).

α3 subunits can co-assemble with β2 or β4 subunits to form functional nAChRs (Sheffield et al., 2000). We found that the α3β4∗ nAChR-selective antagonist α-conotoxin AuIB markedly attenuated the stimulatory effects of nicotine on mHb neurons, as measured using whole-cell recordings, similar to the actions of the broad-spectrum nAChR antagonist mecamylamine. By contrast, equimolar concentrations of the α3β2∗ nAChR-selective antagonist α-conotoxin MII only partially attenuated the effects of nicotine. This suggests that α3β4∗ nAChRs likely to play an important role in regulating the actions of nicotine on habenular neurons, whereas α3β2∗ nAChRs are less involved. Consistent with these observations, infusion of α-conotoxin AuIB into the IPn of rats, at a concentration two-fold higher than that required to block the actions of nicotine in slice recordings, increased their nicotine intake. By contrast, intra-IPn infusion of an equimolar concentration of α-conotoxin MII had no effect on nicotine intake. These data further support a role for α3∗ nAChRs in the habenula-IPn circuit, particularly the α3β4 nAChR subtype, in regulating nicotine intake. It is important to note that local knock-down of α3 subunits in the IPn also increased nicotine intake. The mechanisms by which α3∗ nAChRs expressed by IPn neurons can influence nicotine intake is unclear, but it was recently reported IPn afferents to the laterodorsal tegmental nucleus (LDTg) are activated by nicotine, with this action provoking noxious responses to the drug (Wolfman et al., 2018). Hence, nicotine is likely to stimulate both α3∗ nAChRs located on habenula inputs to the IPn and also those located on IPn afferents to the LDTg and elsewhere in the brain, to elicit nicotine avoidance behaviors and decrease nicotine self-administration behavior (Fig. 5E).

It has been reported that AT-1001, a novel α3β4∗ nAChR antagonist with modest actions at α4β2 or α7 nAChRs, decreased nicotine self-administration in rats after systemic administration (Toll et al., 2012). This finding may appear at odds with the increased nicotine intake reported here in α3∗ nAChR-deficient animals. Although AT-1001 is a potent α3β4∗ nAChR antagonist ($IC_{50}$ ~35 nM), it also inhibits non-nAChR targets, including the serotonin transporter, σ receptors, muscarinic receptors and histamine receptors (Toll et al., 2012). Hence, decreased nicotine intake induced by AT-1001 could reflect actions at non-nAChR targets. The ibogaine derivative 18-methoxycoronaridine (18-MC) is also an α3β4∗ nAChR antagonist and similar to AT-1001 it reduces nicotine intake in rats after systemic administration (Glick et al., 1998), but increases intake after IPn infusion (Glick et al., 2011). Therefore, it is possible that AT-1001 and 18-MC decrease nicotine intake after systemic administration by actions at ganglionic α3∗ nAChRs in the autonomic nervous system. If so, this raises questions about the feasibility of developing α3∗ nAChR agonists or positive allosteric modulators to enhance α3∗ nAChR-mediated transmission in the habenula-IPn circuit for the treatment of tobacco dependence.

In addition to increased risk of tobacco dependence, individuals who carry genetic variation across the *CHRNA5-CHRNA3-CHRNB4* gene cluster are also vulnerable to other neuropsychiatric disorders. For example, the rs1051730 allelic variant in *CHRNA3* is associated with increased risk of alcohol use and abuse (Joslyn et al., 2008) and an interaction of smoking status and body mass (Freathy et al., 2011). Allelic variation at three loci in the intron region (rs112712252, rs190825809, and rs116932868) may protect against opioid dependence (Muldoon et al., 2014). Further, allelic variation in *CHRNA3* is associated with differences in cognitive flexibility (Zhang et al., 2010), externalizing behaviors (Stephens et al., 2012), body mass index (Freathy et al., 2011; Tyrrell et al., 2012), reward deficits (Robinson et al., 2013), and schizophrenia (Petrovsky et al., 2010, 2013). Considering that α3∗ nAChRs are so densely expressed in the mHb-IPn circuit, these human genetics findings hint at broader roles for this circuit beyond tobacco dependence that are relevant to many other neuropsychiatric disorders.

In summary, our findings suggest that α3β4∗ nAChRs regulate the stimulatory effects of nicotine on the mHb-IPn circuit and thereby control nicotine intake (Fig. 5E). Hence, α3β4∗ nAChRs may protect against tobacco addiction by promoting nicotine avoidance behaviors through modulation of the habenula-IPn circuit.

## References

Amos CI, Wu X, Broderick P, Gorlov IP, Gu J, Eisen T, Dong Q, Zhang Q, Gu X, Vijayakrishnan J, Sullivan K, Matakidou A, Wang Y, Mills G, Doheny K, Tsai YY, Chen WV, Shete S, Spitz MR, Houlston RS (2008) Genome-wide association scan of tag SNPs identifies a susceptibility locus for lung cancer at 15q25.1. Nat Genet 40:616–622.

Berrettini W, Yuan X, Tozzi F, Song K, Francks C, Chilcoat H, Waterworth D, Muglia P, Mooser V (2008) Alpha-5/alpha-3 nicotinic receptor subunit alleles increase risk for heavy smoking. Mol Psychiatry 13:368–373.

Boulter J, Evans K, Goldman D, Martin G, Treco D, Heinemann S, Patrick J (1986) Isolation of a cDNA clone coding for a possible neural nicotinic acetylcholine receptor alpha-subunit. Nature 319:368–374.

Caffery PM, Krishnaswamy A, Sanders T, Liu J, Hartlaub H, Klysik J, Cooper E, Hawrot E (2009) Engineering neuronal nicotinic acetylcholine receptors with functional sensitivity to alpha-bungarotoxin: a novel alpha3-knock-in mouse. Eur J Neurosci 30:2064–2076.

Duncan A, Heyer MP, Ishikawa M, Caligiuri SPB, Liu XA, Chen Z, Micioni Di Bonaventura MV, Elayouby KS, Ables JL, Howe WM, Bali P, Fillinger C, Williams M, O'Connor RM, Wang Z, Lu Q, Kamenecka TM, Ma'ayan

A, O'Neill HC, et al. (2019) Habenular TCF7L2 links nicotine addiction to diabetes. Nature 574:372–377.

Fowler CD, Kenny PJ (2014) Nicotine aversion: neurobiological mechanisms and relevance to tobacco dependence vulnerability. Neuropharmacology 76:533–544.

Fowler CD, Lu Q, Johnson PM, Marks MJ, Kenny PJ (2011) Habenular α5 nicotinic receptor subunit signalling controls nicotine intake. Nature 471:597–601.

Frahm S, Slimak MA, Ferrarese L, Santos-Torres J, Antolin-Fontes B, Auer S, Filkin S, Pons S, Fontaine J-F, Tsetlin V, Maskos U, Ibañez-Tallon I (2011) Aversion to nicotine is regulated by the balanced activity of β4 and α5 nicotinic receptor subunits in the medial habenula. Neuron 70:522–535.

Freathy RM, Kazeem GR, Morris RW, Johnson PCD, Paternoster L, Ebrahim S, Hattersley AT, Hill A, Hingorani AD, Holst C, Jefferis BJ, Kring SII, Mooser V, Padmanabhan S, Preisig M, Ring SM, Sattar N, Upton MN, Vollenweider P, Waeber G, et al. (2011) Genetic variation at CHRNA5-CHRNA3-CHRNB4 interacts with smoking status to influence body mass index. Int J Epidemiol 40:1617–1628.

Garcia PD, Gornbein JA, Middlekauff HR (2020) Cardiovascular autonomic effects of electronic cigarette use: a systematic review. Clin Auton Res 30:507–519.

Glick SD, Maisonneuve IM, Visker KE, Fritz KA, Bandarage UK, Kuehne ME (1998) 18-Methoxycoronaridine attenuates nicotine-induced dopamine release and nicotine preferences in rats. Psychopharmacology (Berl) 139:274–280.

Glick SD, Sell EM, McCallum SE, Maisonneuve IM (2011) Brain regions mediating α3β4 nicotinic antagonist effects of 18-MC on nicotine self-administration. Eur J Pharmacol 669:71–75.

Hung RJ, McKay JD, Gaborieau V, Boffetta P, Hashibe M, Zaridze D, Mukeria A, Szeszenia-Dabrowska N, Lissowska J, Rudnai P, Fabianova E, Mates D, Bencko V, Foretova L, Janout V, Chen C, Goodman G, Field JK, Liloglou T, Xinarianos G, et al. (2008) A susceptibility locus for lung cancer maps to nicotinic acetylcholine receptor subunit genes on 15q25. Nature 452:633–637.

Jensen KP, DeVito EE, Herman AI, Valentine GW, Gelernter J, Sofuoglu M (2015) A CHRNA5 smoking risk variant decreases the aversive effects of nicotine in humans. Neuropsychopharmacol 40:2813–2821.

Joslyn G, Brush G, Robertson M, Smith TL, Kalmijn J, Schuckit M, White RL (2008) Chromosome 15q25.1 genetic markers associated with level of response to alcohol in humans. Proc Natl Acad Sci USA 105:20368–20373.

Kenny PJ, Markou A (2006) Nicotine self-administration acutely activates brain reward systems and induces a long-lasting increase in reward sensitivity. Neuropsychopharmacology 31:1203–1211.

Kenny PJ, Chartoff E, Roberto M, Carlezon WA Jr, Markou A (2009) NMDA receptors regulate nicotine-enhanced brain reward function and intravenous nicotine self-administration: role of the ventral tegmental area and central nucleus of the amygdala. Neuropsychopharmacology 34:266–281.

Liu L, Zhao-Shea R, McIntosh JM, Gardner P, Tapper A (2012) Nicotine persistently activates ventral tegmental area dopaminergic neurons via nicotinic acetylcholine receptors containing α4 and α6 subunits. Mol Pharmacol 81:541–548.

Marques-Vidal P, Kutalik Z, Paccaud F, Bergmann S, Waeber G, Vollenweider P, Cornuz J (2011) Variant within the promoter region of the CHRNA3 gene associated with FTN dependence is not related to self-reported willingness to quit smoking. Nicotine Tob Res 13:833–839.

Maskos U, Molles BE, Pons S, Besson M, Guiard BP, Guilloux JP, Evrard A, Cazala P, Cormier A, Mameli-Engvall M, Dufour N, Cloëz-Tayarani I, Bemelmans AP, Mallet J, Gardier AM, David V, Faure P, Granon S, Changeux JP (2005) Nicotine reinforcement and cognition restored by targeted expression of nicotinic receptors. Nature 436:103–107.

Muldoon PP, Jackson KJ, Perez E, Harenza JL, Molas S, Rais B, Anwar H, Zaveri NT, Maldonado R, Maskos U, McIntosh JM, Dierssen M, Miles MF, Chen X, De Biasi M, Damaj MI (2014) The α3β4* nicotinic ACh receptor subtype mediates physical dependence to morphine: mouse and human studies. Br J Pharmacol 171:3845–3857.

Petrovsky N, Quednow BB, Ettinger U, Schmechtig A, Mössner R, Collier DA, Kühn KU, Maier W, Wagner M, Kumari V (2010) Sensorimotor gating is associated with CHRNA3 polymorphisms in schizophrenia and healthy volunteers. Neuropsychopharmacology 35:1429–1439.

Petrovsky N, Ettinger U, Kessler H, Mössner R, Wolfsgruber S, Dahmen N, Maier W, Wagner M, Quednow BB (2013) The effect of nicotine on sensorimotor gating is modulated by a CHRNA3 polymorphism. Psychopharmacology (Berl) 229:31–40.

Rassadi S, Krishnaswamy A, Pié B, McConnell R, Jacob MH, Cooper E (2005) A null mutation for the alpha3 nicotinic acetylcholine (ACh) receptor gene abolishes fast synaptic activity in sympathetic ganglia and reveals that ACh output from developing preganglionic terminals is regulated in an activity-dependent retrograde manner. J Neurosci 25:8555–8566.

Robinson JD, Versace F, Lam CY, Minnix JA, Engelmann JM, Cui Y, Karam-Hage M, Shete SS, Tomlinson GE, Chen TT, Wetter DW, Green CE, Cinciripini PM (2013) The CHRNA3 rs578776 variant is associated with an intrinsic reward sensitivity deficit in smokers. Front Psychiatry 4:114.

Sheffield EB, Quick MW, Lester RA (2000) Nicotinic acetylcholine receptor subunit mRNA expression and channel function in medial habenula neurons. Neuropharmacology 39:2591–2603.

Stephens SH, Hoft NR, Schlaepfer IR, Young SE, Corley RC, McQueen MB, Hopfer C, Crowley T, Stallings M, Hewitt J, Ehringer MA (2012) Externalizing behaviors are associated with SNPs in the CHRNA5/CHRNA3/CHRNB4 gene cluster. Behav Genet 42:402–414.

Stolerman IP, Jarvis MJ (1995) The scientific case that nicotine is addictive. Psychopharmacology (Berl) 117:2–10; discussion 14–20.

Thorgeirsson TE, Geller F, Sulem P, Rafnar T, Wiste A, Magnusson KP, Manolescu A, Thorleifsson G, Stefansson H, Ingason A, Stacey SN, Bergthorsson JT, Thorlacius S, Gudmundsson J, Jonsson T, Jakobsdottir M, Saemundsdottir J, Olafsdottir O, Gudmundsson LJ, Bjornsdottir G, et al. (2008) A variant associated with nicotine dependence, lung cancer and peripheral arterial disease. Nature 452:638–642.

Ting JT, Lee BR, Chong P, Soler-Llavina G, Cobbs C, Koch C, Zeng H, Lein E (2018) Preparation of acute brain slices using an optimized N-methyl-D-glucamine protective recovery method. J Vis Exp. Advance online publicaton. Retrieved February 26, 2018.

Toll L, Zaveri NT, Polgar WE, Jiang F, Khroyan TV, Zhou W, Xie XS, Stauber GB, Costello MR, Leslie FM (2012) AT-1001: a high affinity and selective α3β4 nicotinic acetylcholine receptor antagonist blocks nicotine self-administration in rats. Neuropsychopharmacology 37:1367–1376.

Tuesta LM, Chen Z, Duncan A, Fowler CD, Ishikawa M, Lee BR, Liu X-A, Lu Q, Cameron M, Hayes MR, Kamenecka TM, Pletcher M, Kenny PJ (2017) GLP-1 acts on habenular avoidance circuits to control nicotine intake. Nat Neurosci 20:708–716.

Tyrrell J, Huikari V, Christie JT, Cavadino A, Bakker R, Brion MJ, Geller F, Paternoster L, Myhre R, Potter C, Johnson PC, Ebrahim S, Feenstra B, Hartikainen AL, Hattersley AT, Hofman A, Kaakinen M, Lowe LP, Magnus P, McConnachie A, et al. (2012) Genetic variation in the 15q25 nicotinic acetylcholine receptor gene cluster (CHRNA5-CHRNA3-CHRNB4) interacts with maternal self-reported smoking status during pregnancy to influence birth weight. Hum Mol Genet 21:5344–5358.

Wada E, Wada K, Boulter J, Deneris E, Heinemann S, Patrick J, Swanson LW (1989) Distribution of alpha 2, alpha 3, alpha 4, and beta 2 neuronal nicotinic receptor subunit mRNAs in the central nervous system: a hybridization histochemical study in the rat. J Comp Neurol 284:314–335.

Ware JJ, van den Bree MBM, Munafò MR (2011) Association of the CHRNA5-A3-B4 gene cluster with heaviness of smoking: a meta-analysis. Nicotine Tob Res 13:1167–1175.

Wolfman SL, Gill DF, Bogdanic F, Long K, Al-Hasani R, McCall JG, Bruchas MR, McGehee DS (2018) Nicotine aversion is mediated by GABAergic interpeduncular nucleus inputs to laterodorsal tegmentum. Nat Commun 9:2710.

Xu W, Gelber S, Orr-Urtreger A, Armstrong D, Lewis RA, Ou CN, Patrick J, Role L, De Biasi M, Beaudet AL (1999) Megacystis, mydriasis, and ion channel defect in mice lacking the alpha3 neuronal nicotinic acetylcholine receptor. Proc Natl Acad Sci USA 96:5746–5751.

Yeh JJ, Yasuda RP, Dávila-García MI, Xiao Y, Ebert S, Gupta T, Kellar KJ, Wolfe BB (2001) Neuronal nicotinic acetylcholine receptor alpha3 subunit protein in rat brain and sympathetic ganglion measured using a subunit-specific antibody: regional and ontogenic expression. J Neurochem 77:336–346.

Zhang H, Kranzler HR, Poling J, Gelernter J (2010) Variation in the nicotinic acetylcholine receptor gene cluster CHRNA5-CHRNA3-CHRNB4 and its interaction with recent tobacco use influence cognitive flexibility. Neuropsychopharmacology 35:2211–2224.